

# Accurate Diagnosis of COVID-19 from Self-Collectable Biospecimens Using Synthetic Apolipoprotein H Peptide-Coated Nanoparticle Assay

Junwon Kang, Haewook Jang, Tae Hyun Kim, Untack Cho, Hyeon Bang, Jisung Jang, Wooseok Lee, Hyelyn Joo, Jinsung Noh, Gi Yoon Lee, Dong Hoon Shin, Chang Kyung Kang, Pyoeng Gyun Choe, Nam Joong Kim, Myoung-don Oh, Manki Song, Sunghoon Kwon,\* Francisco Veas,\* and Wan Beom Park\*



Cite This: <https://doi.org/10.1021/acs.analchem.2c03813>



Read Online

ACCESS |



Metrics & More

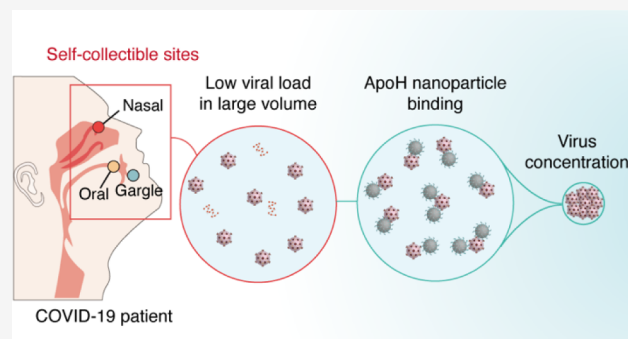


Article Recommendations



Supporting Information

**ABSTRACT:** A high-throughput, accurate screening is crucial for the prevention and control of severe acute respiratory syndrome coronavirus 2 (SARS-CoV-2). Current methods, which involve sampling from the nasopharyngeal (NP) area by medical staffs, constitute a fundamental bottleneck in expanding the testing capacity. To meet the scales required for population-level surveillance, self-collectable specimens can be used; however, its low viral load has hindered its clinical adoption. Here, we describe a magnetic nanoparticle functionalized with synthetic apolipoprotein H (ApoH) peptides to capture, concentrate, and purify viruses. The ApoH assay demonstrates a viral enrichment efficiency of >90% for both SARS-CoV-2 and its variants, leading to an order of magnitude improvement in analytical sensitivity. For validation, we apply the assay to a total of 84 clinical specimens including nasal, oral, and mouth gargles obtained from COVID-19 patients. As a result, a 100% positivity rate is achieved from the patient-collected nasal and gargle samples, which exceeds that of the traditional NP swab method. The simple 12 min pre-enrichment assay enabling the use of self-collectable samples will be a practical solution to overcome the overwhelming diagnostic capacity. Furthermore, the methodology can easily be built on various clinical protocols, allowing its broad applicability to various disease diagnoses.



## INTRODUCTION

Despite the varying levels of public health efforts being made to prevent the rapid spread of severe acute respiratory syndrome coronavirus 2 (SARS-CoV-2), a considerable number of new infected cases and deaths continue to arise globally.<sup>1</sup> Since the World Health Organization declared coronavirus disease 2019 (COVID-19) outbreak as a pandemic, various forms of vaccines and therapeutic reagents have been actively developed and clinically validated for emergency use approval.<sup>2</sup> However, the emergence and rapid succession of new variants along with growing evidences showing that some mutated types often evade immune responses produced by prior vaccinations or infections raise concerns existentially.<sup>3</sup> As the social and economic burdens extend, demands and attempts to gradually reopen business and schools regardless of the recurrent outbreak have become inevitable.

To effectively contain the local viral transmission, while returning to daily life, large-scale diagnostic tests to identify, trace, and isolate infected individuals are mandated.<sup>4,5</sup> The

current standards to detect SARS-CoV-2 involve testing nasopharyngeal (NP) swab samples using quantitative reverse transcription-polymerase chain reaction (RT-qPCR).<sup>6</sup> Approaches using isothermal amplification or extraction-free methods have been proposed, with emphasis on simplifying the procedure and reducing the turnaround time.<sup>7–9</sup> However, the delay in obtaining test results mainly occurs not only in the time required for a single assay. More importantly, the overall capacity to sample and perform multiplexed reactions appears to be a great hurdle for regular base population-level screening.<sup>10,11</sup> Due to the quality of specimens, which highly depends on the proper swabbing technique and safety issues, NP swab sampling requires the assistance of trained

**Received:** August 31, 2022

**Accepted:** November 2, 2022

**Published:** November 18, 2022

professionals.<sup>12</sup> Consequently, this leads to an increase in the wait time and gatherings at each testing location which also escalates the risk of exposure to SARS-CoV-2. On the other hand, the absence of medical staffs being reassigned to areas to support COVID-19 severely disrupts the general healthcare services.

Diagnostic tests utilizing self-collectable samples such as nasal swab, oral swab, saliva, or mouth gargle are being evaluated as potential alternatives to resolve the accessibility and throughput constraints, negating the needs for human-to-human interactions, and improve patient compliance.<sup>10,13–19</sup> In spite of these advantages, the viral load associated with disease progression and severity is typically low,<sup>14–16</sup> which constitutes the possibility of generating false-negative results. Recently, some studies have shown that self-collectable specimens often have similar or higher viral material compared to the NP swabs.<sup>10,17,18</sup> However, it has been found that the total viral load can vary dynamically, not only between sampling locations, but also according to the time of collection after infection.<sup>19–21</sup> Along with these studies, several attempts have been made to improve the analytical sensitivity or testing capacity, for instance, utilizing next-generation sequencing;<sup>11</sup> however, the additional time and cost required per operation have hindered their widespread clinical adoption for SARS-CoV-2 diagnosis. To expedite the use of self-collectable samples to our current COVID-19 screening practice as an NP substitute, continuous efforts to enhance the assay sensitivity accompanied by the exploration of the correlation of viral loads between sampling sites are necessary.

In this study, we present a synthetic apolipoprotein H (ApoH) peptide-coated magnetic nanoparticle that can efficiently bind to live viruses. Considering that biological specimens are eluted and stored in 2–4 mL of viral transport media prior to RT-qPCR and the maximum reaction volume of a typical PCR machine used in clinical laboratories is around <100  $\mu$ L per slot, in practice, only 2.5–5% of the total samples is subjected for testing. We use the ApoH nanoparticle assay to capture, purify, and concentrate viral particles and demonstrate the detection of SARS-CoV-2 with a 10-fold increase in analytical sensitivity. The synthetic ApoH peptide-coated nanoparticle differs from other immunomagnetic based strategies such as antibody-coated nanobeads as it can bind to and cover a wide range of viral species including its variants. Next, we measure the viral loads from the nasal and oral swabs and mouth gargles collected by the patients themselves along with NP and oropharyngeal (OP, throat) swabs taken by healthcare workers simultaneously. We discover that the total viral load obtained from the self-collectable specimens is, on average, significantly lower than that of the NP swab samples which have, so far, questioned its clinical adoption. However, by applying the assay, we realize a 100% positivity rate of detecting SARS-CoV-2 from both patient-collected nasal swab and mouth gargles which were unable to achieve even through conventional NP swab-based testing methods, regardless of the large variation of the sample collection quality. Our work finally provides a pragmatic solution of implementing self-collection of biospecimens into current COVID-19 testing standards by overcoming the false-negative concerns. Moreover, with the unique binding characteristics of the synthetic ApoH peptide to a broad spectrum of viruses, ultimately, the assay will resolve the capacity limit of diagnosis for COVID-19 as well as for the forthcoming pandemic and infectious diseases.

## EXPERIMENTAL SECTION

**Clinical Specimen Collection.** Clinical samples were obtained from hospitalized patients, who were confirmed positive for SARS-CoV-2, after obtaining informed consent for research testing that complied with the ethical regulations under an Institutional Review Board (IRB)-approved protocol (2009-098-1157) at the Seoul National University Hospital (SNUH). Written informed consent was obtained from all patients. All specimens including NP, OP, nasal, and oral swab samples and mouth gargles were collected at the same time and stored at 4 °C before processing. NP and OP swab samples were collected by clinicians, whereas the nasal and oral swabs and mouth gargles were obtained by the patients themselves. NP swabs were taken from the posterior nasopharynx via the nostril, whereas the OP swabs were taken from the pharyngeal tonsil and posterior pharynx, excluding the tongue. The swabs were slowly rotated in place, removed, and inserted in a transfer tube containing 2 mL of 0.9% PBS (10010-023, Gibco). For the self-collectable nasal and oral swab samples, all participants were first asked to clean their hands and cough three to five times. The patients were then asked to gently insert the swab either into the nostril (nasal) or the floor of the mouth (oral), including the outer gums and inside the cheeks, and slowly rotate 10 times. Then, similar to the NP and OP specimens, these swabs were inserted into a transfer tube. Finally, in the case of mouth gargles, the patients were instructed to hold 10 mL of saline solution in their mouth, gargle the solution for 5 s and repeat by tilting their head back, and expel the content into an empty 50 mL sterile tube.

### SARS-CoV-2 Enrichment Using ApoH Nanoparticles.

ApoH nanoparticles and a custom capture buffer (75  $\mu$ L used for 1 mL of sample) were added to the sampled specimen and gently mixed by inverting the tube three times. The primary role of the capture buffer was to ensure that the solution was kept at neutral pH. Considering the isoelectric point of SARS-CoV-2 and its variants,<sup>22</sup> these viruses bear negative charge at pH = 7. As the functional region of the ApoH peptide presents a positive charge on its surface, a tight control of the solution's pH to neutrality was important. The samples were placed in a thermomixer (KTM-100C, KBT), set at 4 °C with a rotation speed of 800 rpm, for 5 min to enable an efficient binding of ApoH nanoparticles to the virions. Next, the sample tubes were placed in a magnetic rack (DynaMag Magnet, Invitrogen) for 5 min for particle enrichment. After removing the supernatant, the magnet was removed, and the remaining content consisting of ApoH-bound viral particles was used for the following RNA extraction and RT-qPCR. In the case of mouth gargles, the samples were treated with 3% NAC solution (850  $\mu$ L used for 1 mL of sample, A7250, Sigma) and incubated for 30 min at 37 °C prior to the virus enrichment procedure mentioned above.

**RNA Extraction and RT-qPCR.** Following virus enrichment, RNA was extracted using the QIAamp Viral RNA Mini kit (Qiagen) according to the manufacturer's instruction. In brief, the ApoH particle-bound viruses were resuspended using 560  $\mu$ L of lysis buffer and incubated for 10 min at 37 °C. Next, the solution was placed in a magnetic rack for 5 min. The supernatant containing the viral nucleic acids, separated from the ApoH nanoparticles, was collected and purified. Finally, the extracted RNA was eluted and stored at –70 °C before analysis. RT-qPCR was performed using the QPLEX COVID-19 test (QMCOVID02, QuantaMatrix Inc.). A mixture containing 10  $\mu$ L of 2 $\times$  One-step Premix, 5  $\mu$ L of Oligo

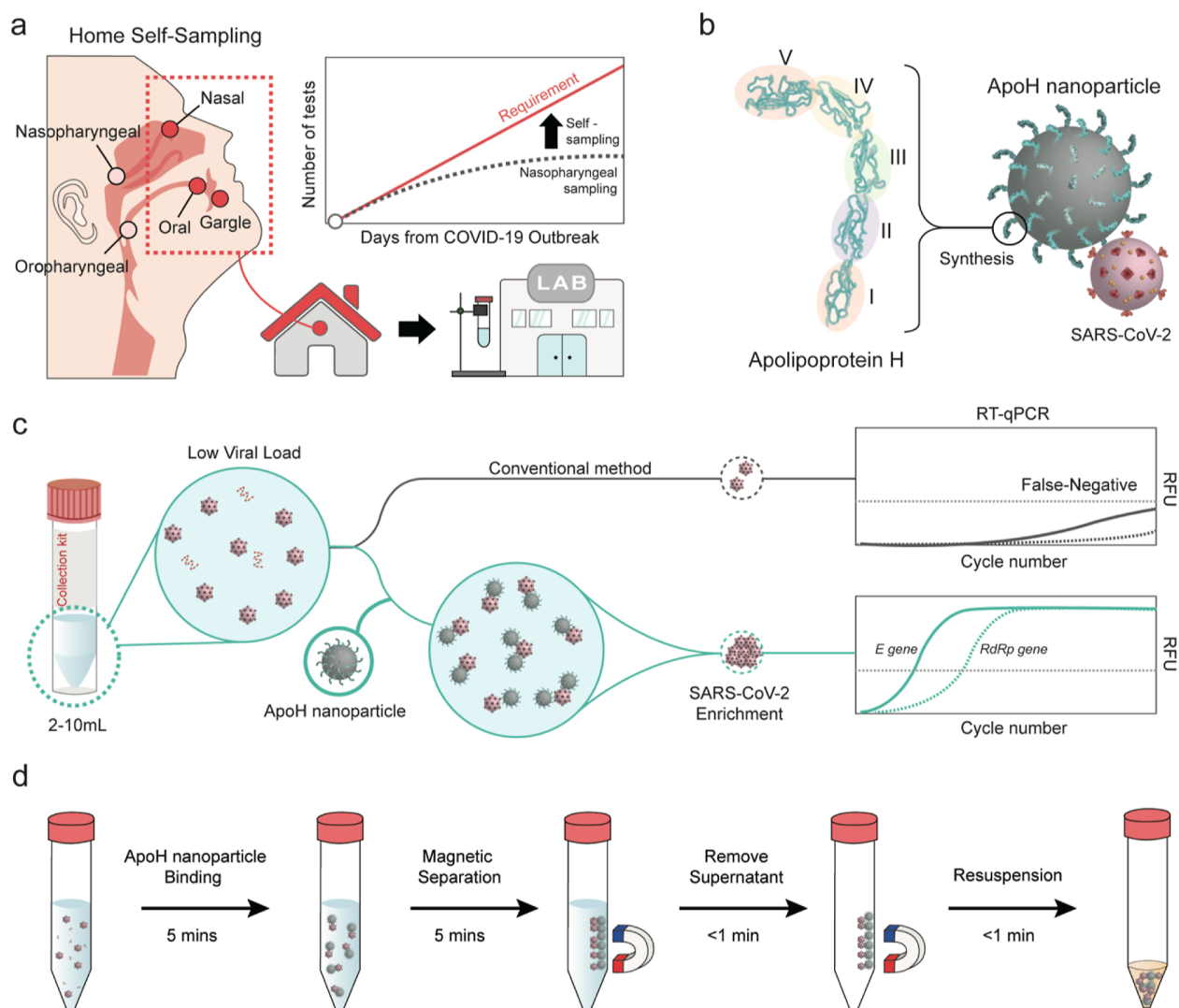


**Figure 1.** Schematic of SARS-CoV-2 enrichment procedure using ApoH nanoparticles. (a) Virus sampling locations available for COVID-19 testing. Samples that can be self-collected are outlined in red. (b) Molecular structure of the ApoH protein (left) and illustration of a synthetic ApoH peptide-coated nanoparticle bound to a SARS-CoV-2 virion (right). (c) Strategy to enhance the virus detection efficiency. The total amount of viruses in the sampled specimen can be concentrated using ApoH nanoparticles, overcoming the traditional RT-qPCR volume limit, which results in the increase of analytical sensitivity and detection rate. (d) SARS-CoV-2 enrichment workflow. The entire procedure consists of ApoH nanoparticle binding, magnetic separation, and removal of the supernatant to concentrate and collect the viruses. The total time required for the enrichment assay is less than 12 min, and the entire viral detection procedure is completed within 2 h.

Mix, and 5  $\mu\text{L}$  of RNA sample was prepared and used for complementary DNA (cDNA) synthesis using reverse transcription and amplification of the target genes in the same reaction tube. The primer and probe sets used in the kit were designed to target the RdRp and E genes of SARS-CoV-2. Of note, the primers were applied to 22 different types of other respiratory viruses and bacteria to test the specificity of the assay (Table S1). After five cycles of pre-amplification, the product was subjected to 35 cycles of PCR for measurement. The positivity of infection was defined when both RdRp and E genes were detected; inconclusive when either gene target was detected; and negative when both were undetectable.<sup>25</sup>

## RESULTS

### Design and Synthesis of ApoH-Coated Nanoparticles.

The ApoH protein, also known as beta-2 glycoprotein 1, is a plasma glycoprotein which is predominantly expressed in the liver. Although, the functions of ApoH are not yet fully

understood, it appears to be involved in blood coagulation pathways and immune responses.<sup>24</sup> An interesting property of ApoH is that it interacts with hydrophobic or negatively charged substances with high affinity, such as anionic phospholipids, heparin, activated platelets, and apoptotic cells.<sup>25–28</sup> Also, we and others have previously shown that ApoH binding frequently occurs with infectious agents like bacteria or viruses, making the protein promising for use in various diagnostic approaches.<sup>29,30</sup> Inspired by these aspects, a synthetic ApoH peptide was designed and engineered by mimicking the corresponding functional regions of the ApoH protein. In this form, the size and the molecular complexity of the virus-binding domain were minimized, allowing the ApoH peptide to be densely packed to functionalized surfaces, resulting in a 27.29% improvement in the virus capture efficiency (Figure S1). Moreover, the protein-by-protein variation was controlled, allowing reliability and repeatability in its production. The synthesized peptide was then attached



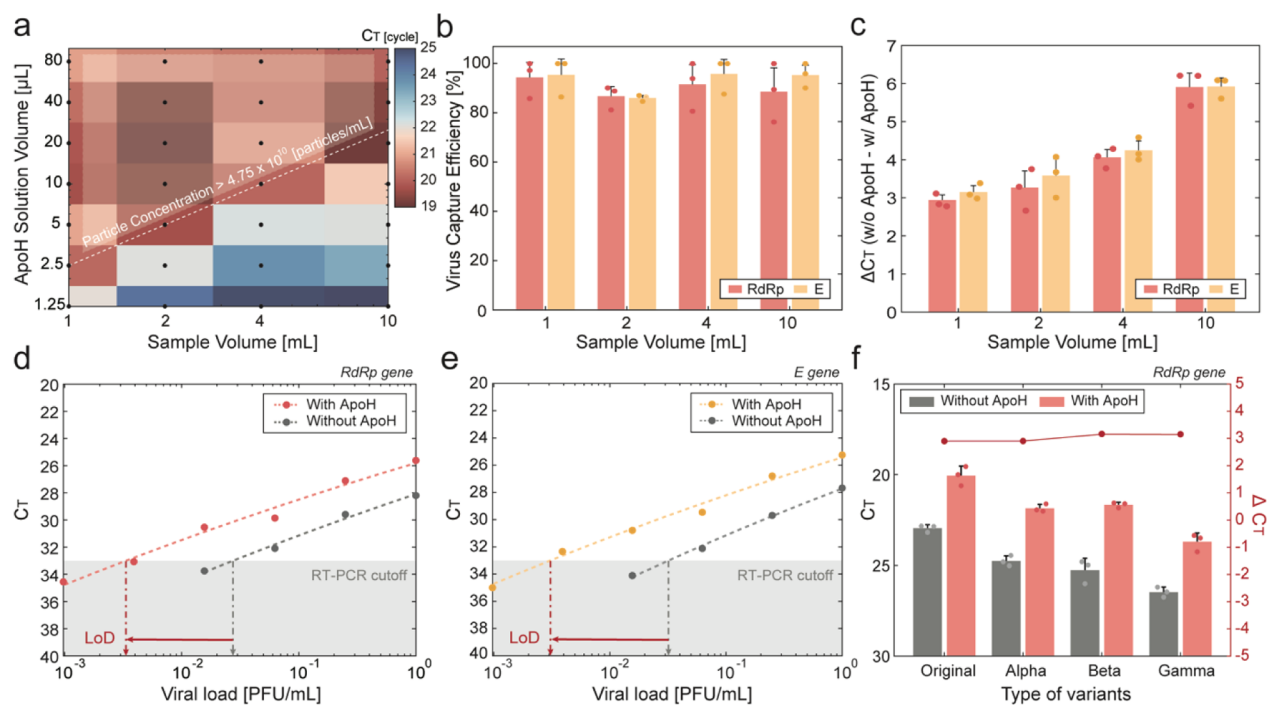


**Figure 2.** Characterization of SARS-CoV-2 enrichment performance of ApoH nanoparticles. (a) Optimization of the ApoH nanoparticle concentration for SARS-CoV-2 capture. (b) Virus capture efficiency as a function of processing volume. A constant amount of 125 PFU viruses are spiked into different volumes of solution. (c) Improvements in the C<sub>T</sub> value after applying the ApoH assay to varying amounts of sample volume. Samples are spiked with a constant concentration of 125 PFU/mL viruses. ΔC<sub>T</sub> is calculated by subtracting the C<sub>T</sub> values from each enrichment test to the C<sub>T</sub> value obtained from a 140 μL sample, which represents the conventional RT-qPCR procedure. Comparison between the RT-qPCR detection limit, with and without using the ApoH nanoparticles, for (d) RdRp and (e) E genes. (f) Variant independent binding of ApoH nanoparticles. The average ΔC<sub>T</sub> of RdRp gene for each alpha, beta, and gamma variant after ApoH enrichment is presented in a line plot (red) above.

and functionalized to magnetic nanoparticles of a mean diameter of 200 nm. The ApoH nanoparticles were used for SARS-CoV-2 enrichment following a simple protocol which consists of ApoH particle binding and magnetic separation (Figure 1). During the virus-binding process, a capture buffer was added to the solution to support the viral capture and cell lysis to extract the virus from the infected cells for enrichment.

**SARS-CoV-2 Enrichment Using ApoH-Coated Nanoparticles.** To optimize the viral enrichment procedure, mixtures of different volume ratios of solutions containing ApoH nanoparticles ( $1.9 \times 10^{10}$  particles/μL) to samples spiked with 125 plaque-forming units (PFUs) of SARS-CoV-2 virions in diethylpyrocarbonate (DEPC)-treated water were prepared. After collecting the viruses following ApoH nanoparticle binding (Figure S2) and magnetic separation, each sample was subjected to RT-qPCR to estimate the recovery rate. The primers used in the reaction were designed to specifically target the RNA-dependent RNA polymerase (RdRp) and envelope (E) genes (Table S1 and Figure S3). As a result, a particle concentration above  $4.75 \times 10^{10}$  particles/mL was determined to be deemed optimal for efficient virus retrieval (Figure 2a).

To quantitatively assess the volume-dependent virus capture efficiency, a fixed number of 125 PFU virions was again dispensed into varying amount of sample volume ranging from 1 to 10 mL (Figure 2b). Using the optimized concentration of ApoH nanoparticles for capture, the C<sub>T</sub> values of each sample were measured before and after the enrichment process. The total number of RNA copies was derived from C<sub>T</sub> values by converting a single infectious unit (PFU) to  $1 \times 10^4$  copies of

viral RNA to calculate the capture efficiency.<sup>31</sup> In total, an average of  $90.32 \pm 2.90\%$  and  $93.20 \pm 4.12\%$  capture efficiency was achieved for RdRp and E gene, respectively, revealing the successful recovery of virus, regardless of the processing volume. Similar results were also derived through a different quantification method based on the plaque assay, showing a total capture efficiency of  $96.0 \pm 4.45\%$  (Figure S4).

Next, to demonstrate the viral concentration using the ApoH assay for improved COVID-19 detection accuracy, a solution containing 125 PFU/mL of SARS-CoV-2 was divided into aliquots of 1, 2, 4, and 10 mL and tested (Figure 2c). Compared to the C<sub>T</sub> cycles obtained from a 140 μL suspension which refers to the maximum volume that a conventional PCR machine can accommodate, a substantial reduction in C<sub>T</sub> value was observed with the increasing sample volume used. The increase in ΔC<sub>T</sub> verifies that the loss of viral RNA due to limited reaction volume during RT-qPCR can be significantly reduced through the viral concentration. Finally, the limit of detection (LoD) of the assay was evaluated (Figure 2d,e). Based on the 33 cycles defined as the PCR cutoff, a 10-fold increase in analytical sensitivity was achieved. In addition, the ApoH assay was performed against several SARS-CoV-2 mutations, including the alpha, beta, and gamma variants (Figures 2f and S5). Each type of viruses was spiked in 2 mL of DEPC-treated water at a concentration of approximately 12.5 PFU/mL and processed. Similar to the original COVID-19 virus, the ApoH nanoparticles efficiently bound to all variants, exhibiting an average C<sub>T</sub> reduction of  $3.04 \pm 0.14$  and  $3.12 \pm 0.27$  for RdRp and E gene, respectively. The variant-independent binding behavior illustrates the broad applicability

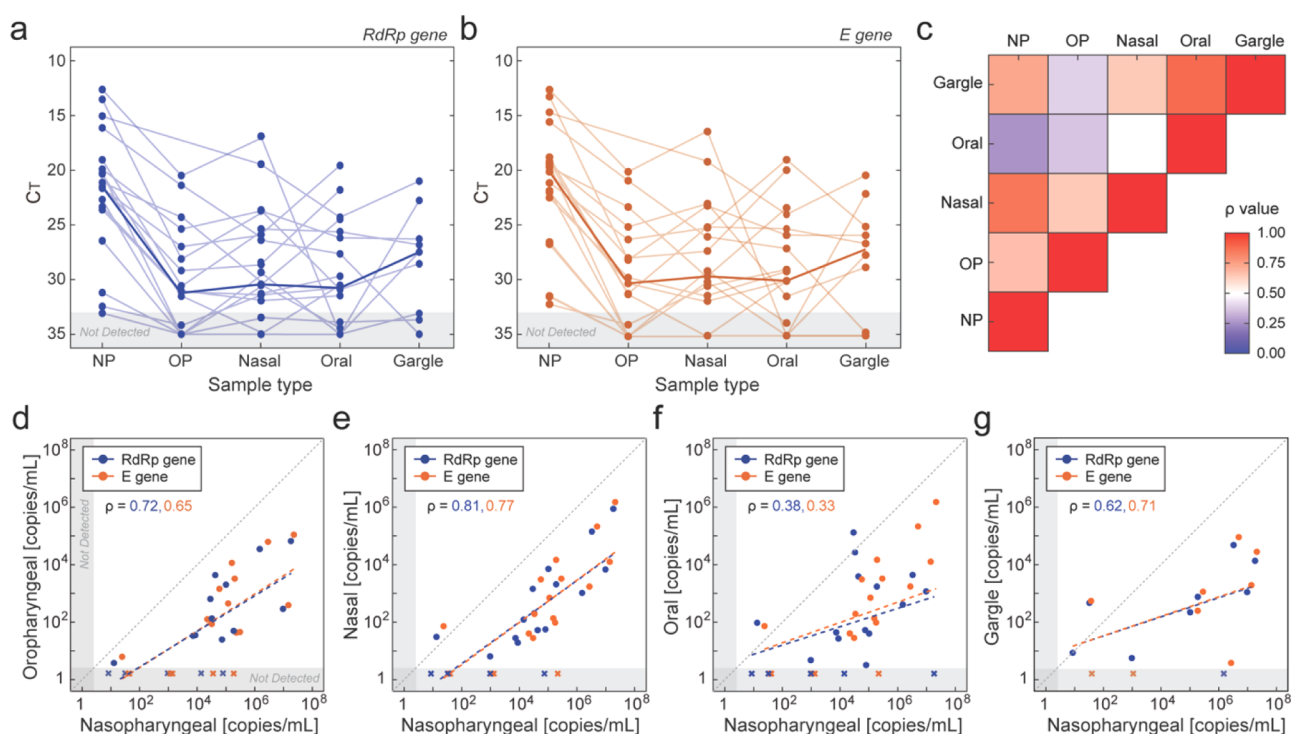


**Figure 3.** Correlation of viral loads between sampling sites. Matched-paired viral loads of NP, OP, nasal, and oral swabs and mouth gargles measured using (a) RdRp and (b) E genes. Bold line indicates the median viral load obtained from each sampling location. (c) Heatmap of correlation coefficient between sample types. Viral RNA copy number from (d) OP ( $n = 18$ ), (e) nasal ( $n = 19$ ), (f) oral swab ( $n = 19$ ), and (g) mouth gargles ( $n = 9$ ) compared to NP swab samples. Each data point reflects samples that are collected from the same patient at the same time. Regression lines for RdRp and E genes are expressed in blue and orange dotted lines, respectively.  $\rho$  represents Spearman's rank correlation coefficient.

and efficacy of the ApoH assay for the sensitive diagnosis of viral infections.

Before applying the assay directly to clinical specimens, the viral enrichment procedure was validated using nasal swab, oral swab, and mouth gargles obtained from healthy individuals. Here, mouth gargles were chosen over saliva due to the ease of collection, patient comfort, and to neglect the additional preprocessing steps required to digest the residual substances such as sputum (Figure S6). Considering that the majority of viruses from COVID-19 patients reside within the cells infected through continuous replication and propagation (assumed to be around  $10^5$  virions per cell),<sup>32</sup> first, the cell lysis efficiency of the capture buffer was inspected (Figure S7a,b). The capture buffer of 150  $\mu\text{L}$  was added to 2 mL of phosphate-buffered saline (PBS) containing  $2 \times 10^6$  of Vero cells and slightly vortexed. A portion of cells was sequentially sampled after 5, 10, 30, and 60 min to observe the amount of cell membrane rupture using a live/dead viability assay. An average of >99% of cells was completely permeable within 5 min, allowing the viruses to be extracted and exposed in suspension for ApoH nanoparticle binding. Next, each nasal and oral swab was eluted in 2 mL of PBS, and mouth gargles were collected by rinsing out 10 mL of saline solution in an empty 15 mL sterile tube. PBS was selected as a sample collection and transport medium based on the 4 day virus preservation test at 4 °C in which negligible amount of RNA degradation was observed (Figure S8). To mimic the presence of viral infection in SARS-CoV-2 patients, 125 PFUs of live viruses were spiked into these samples for the test. Here, the amount of ApoH nanoparticles was slightly adjusted to a concentration of  $1.9 \times 10^{11}$  particles/mL to ensure sufficient

binding to viruses which may be affected by impurities such as epithelial cells. As expected, a significant decrease in C<sub>T</sub> values was noticed in all sample types after viral concentration (Figure S7c–e).

#### Clinical Validation of the ApoH Nanoparticle Assay.

Following the ApoH nanoparticle characterization, the assay was applied to a total of 84 clinical specimens obtained from 19 hospitalized patients who were confirmed positive to SARS-CoV-2 infection. Based on the patient consent available, NP and OP swabs sampled by medical staff members as well as nasal swab, oral swab, or mouth gargles collected by the patient themselves were subjected to the test. Similar to the approach above, the swab samples were eluted in 2 mL of PBS, and mouth gargles were collected after rinsing out 10 mL of saline solution in a 15 mL tube. However, this time, 140  $\mu\text{L}$  of the sampled specimens was separated and directly ran through RT-qPCR, following the current diagnostic procedure used for COVID-19 detection, and later, the remaining volume was used for ApoH capture. All samples were processed within 6 h upon collection.

To investigate the correlation between the sampling sites and determine the potential candidate among the self-collected specimens that could be used to diagnose SARS-CoV-2 most effectively, the viral loads from the 140  $\mu\text{L}$  aliquots were analyzed in pairs (Figure 3a–c). Within the patient cohort studied, the average viral loads found in the self-collected nasal swab, oral swab, and mouth gargles were substantially low compared to the matched NP samples (Figure 3d–g). Surprisingly, even in OP swabs, which are often used in some COVID-19 screening kits, the number of viral materials was only comparable to the self-collected nasal swabs.

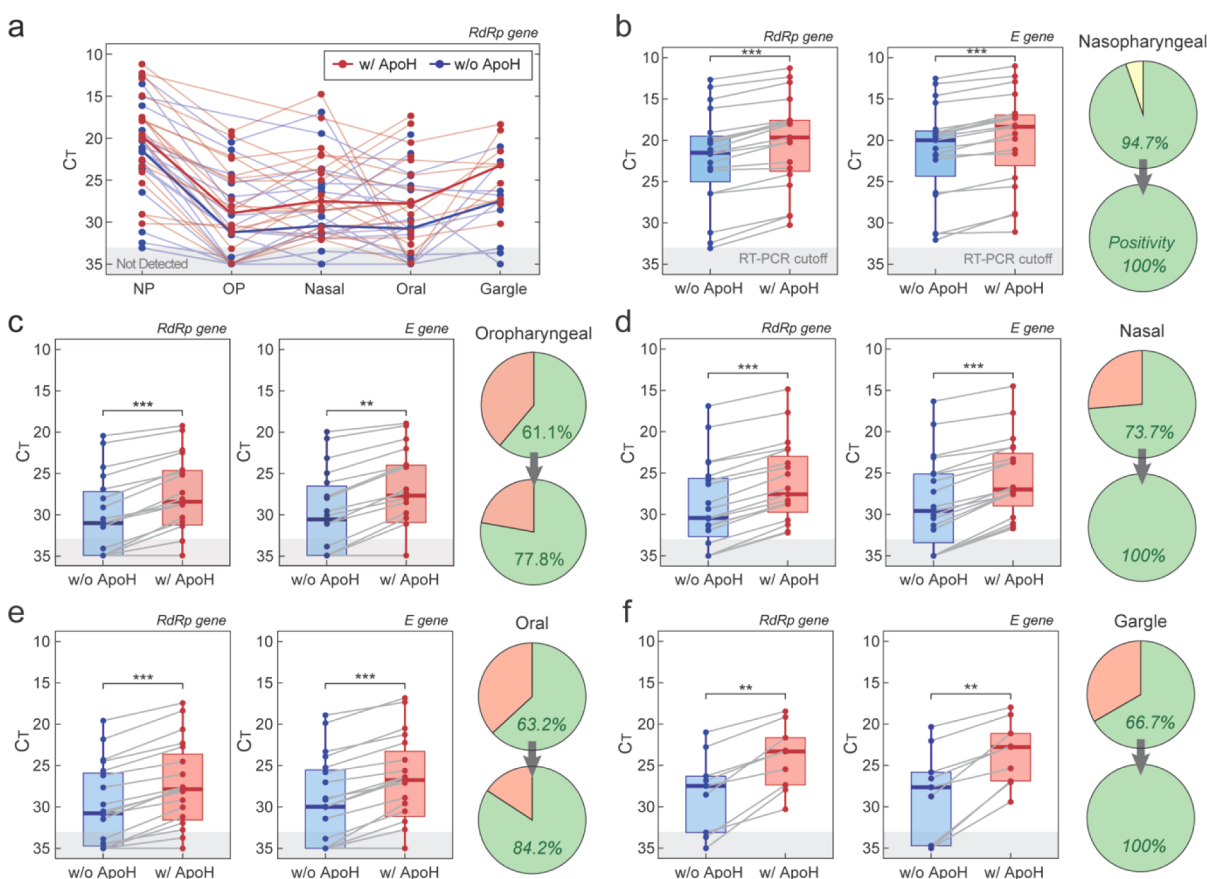


**Figure 4.** Diagnosis of COVID-19 from hospitalized patients using the ApoH assay. (a) Comparison between matched-paired  $C_T$  values of the RdRp gene measured from NP, OP, nasal, and oral swabs, and mouth gargles, with (red) and without (blue) applying the ApoH assay. Bold line indicates the median  $C_T$  values obtained from each sampling location. Change in  $C_T$  values and COVID-19 positivity rate from (b) NP ( $n = 19$ ), (c) OP ( $n = 18$ ), (d) nasal ( $n = 19$ ), and (e) oral ( $n = 19$ ) swabs and (f) mouth gargle ( $n = 9$ ), with and without using the ApoH assay. Paired samples are connected in lines. The gray area represents the PCR cutoff of  $C_T = 33$ . Green, orange, and yellow areas in the pie chart indicate the proportion of positive, negative, and inconclusive test results, respectively. ( $p$ -values: \*\*  $< 0.01$ ; \*\*\*  $< 0.001$ , the Wilcoxon signed-rank test).

Considering the relation to the NP specimen, the highest correlation was found in the nasal swab samples. As a result, a higher number of false-negatives were observed in all samples compared to the NP specimen. However, in the case of mouth gargles, given that only 1.4% of the sample volume was analyzed, the total amount of virus contained in the 10 mL collection was estimated to be comparable to the NP swab samples.

Finally, the ApoH nanoparticles were applied to the remaining swab samples and mouth gargles of 1.84 and 9.86 mL, respectively, to evaluate the accuracy and enhancement of detecting COVID-19 compared to the traditional RT-qPCR method measured from the 140  $\mu$ L aliquots (Figures 4a and S9). The  $C_T$  values from all samples decreased significantly, demonstrating the benefit of ApoH nanoparticles for improved analytical sensitivity. The largest difference in  $C_T$  values was shown in mouth gargles, particularly due to the increased sampling volume of 10 mL, compared to the swab specimens. Interestingly, the virus concentration using the ApoH assay was more efficiently analyzed in samples with lower viral loads (Figure S10). The noticeable difference in  $C_T$  numbers also led to changes in positivity rate for COVID-19 detection (Figure 4b–f). The incidence of false-negative cases decreased dramatically from all sampling locations. Specifically, for the NP swab, nasal swab, and gargle samples, 5.3, 26.3, and 33.3%

of the false-negative cases, respectively, all turned positive after applying the ApoH assay.

## DISCUSSION

Despite various strategies that are being developed to improve the throughput for COVID-19 diagnosis, the sampling procedure which involves NP swabbing constitutes a huge barrier of scaling up the overall testing capacity. We explore the possibility of utilizing self-collectable specimens that could easily be acquired noninvasively from home, to avoid the needs of timely in-person visits to designated examination areas, mitigating the fundamental hurdles of population-level screening. The synthetic ApoH nanoparticle we describe enables the sensitive capture and concentration of live viruses from diluted biological specimens which significantly increase the number of virions subjected to RT-qPCR analysis. The improvements made through the simple 12 min protocol allow a 10-fold increase in analytical sensitivity compared to the regular RT-qPCR process performed without prior enrichment steps, permitting the accurate diagnosis of SARS-CoV-2 from the nasal and oral swab and gargle samples which typically suffer from insufficient viral loads. Surprisingly, by testing the nasal swab or mouth gargles collected by COVID-19 patients themselves, the ApoH assay shows a 100% detection rate which outperforms the use of conventional NP swab-based testing methods.



Various types of self-collectable biospecimens have been exploited for their use in SARS-CoV-2 diagnosis. However, due to the lack of standardized protocols, differing groups of patient cohorts, and samples being tested between studies, the optimal sampling site that holds the largest, stable amount of viral material has remained unclear.<sup>16,33</sup> From our matched-paired analysis, swabs taken from the nasal cavity revealed the highest correlation in viral load to the NP area, at the same time, demonstrating the lowest false-negative rate of 26.3%. However, the fact that the detection rate cannot be reached up to the level of NP specimen, even from the nasal swab sample itself, questions the adoption of using self-collectable specimens for clinical purposes. On the other hand, using the ApoH assay, the amount of viral material has significantly been increased, particularly in mouth gargles which instantly became comparable to the NP swabs. The effect of virus concentration has most apparently been observed in gargles due to the large collection volume. Consequently, together with nasal swabs, the false-negative rate from using mouth gargles decreased dramatically down to 0%, presenting potentials as a NP swab substitute.

Although the approach in our study focuses on utilizing self-collectable biospecimens, the ApoH assay can also be selectively applied to and benefit the most widely used NP-based testing methods in situations where the test accuracy is critical. Recent studies have revealed that the false-negative rate produced by NP swab samples can range from 15–30%, which is yet considered high regarding the disease infectivity.<sup>34,35</sup> This percentage further increases during the presymptomatic phase in which the viral material is relatively insufficient but highly contagious.<sup>36</sup> Also, unlike previously emerged coronaviruses, epidemiological studies have indicated that the infectious period for SARS-CoV-2 frequently begins prior to the symptom onset, approximately 2 days after the initial exposure, making the disease highly transmissible.<sup>37</sup> Thus, failures to identify such pauci-symptomatic or even asymptomatic subjects during the early spread can lead to an explosive transmission of SARS-CoV-2 through super-spreaders.<sup>36,38</sup> Furthermore, the occurrence of false-negative results can raise particular concerns in places such as hospitals or intermediate care facilities, where a group of high-risk individuals are present. Studies have shown that vulnerable patients with older age, comorbidities, impaired immune function, or pregnancy are found to contain low viral loads due to their prolonged nuclear acid conversion (viral shedding).<sup>39,40</sup> Therefore, sensitivity improvements made by implementing the ApoH assay to the standard NP-based surveillance tests can contribute to mitigate the local surge of COVID-19 and prevent the collapse of the overall healthcare systems.

With efforts to reduce the cost and number of RT-qPCR for population-level screening, several pooling strategies have been proposed and developed to scale up the COVID-19 testing capacity.<sup>11,41</sup> However, as each pool contains multiple samples in a single pot, it seems inevitable to dilute the viral loads contained in individual specimens. This inherently restricts the available number of samples being included in a single pool. We propose that the ApoH assay can address the trade-off between the analytical sensitivity and throughput caused by the PCR volume limit. Taking into account that the current NP swab testing methods utilize a specimen volume of around 20–100  $\mu\text{L}$  per reaction, the successful demonstration of concentrating viruses from a 10 mL mouth gargle implies

that a total number of samples of more than 2 orders of magnitude can be pooled together and processed without sacrificing the sensitivity. This opens up opportunities to realize the pooled-test method for accurate screening and massive surveillance tests.

## CONCLUSIONS

As the disease evolves and spread continues, emphasis is being placed on establishing new strategies or examination guidelines to overcome the capacity limit of current COVID-19 screening practices. In this regard, the capability to diagnose SARS-CoV-2 using self-collectable specimens and to perform multiplexed sample reaction without affecting the test accuracy using the ApoH assay can be a practical solution for a scalable surveillance option. To accelerate the deployment of our technology to clinical fields, further validation over extended patient cohorts must be followed. Nevertheless, from the results featuring higher enrichment efficiency at lower viral loads, we anticipate that the ApoH assay will also be able to accommodate groups of presymptomatic patients that were considered difficult to be diagnosed using conventional methods. Finally, beyond SARS-CoV-2 and its variants, the high affinity of ApoH nanoparticles against a variety of viruses and pathogens, allows us to easily expand our approach to multiple diseases including future species with pandemic potential and also integrate with other clinical protocols.

## ASSOCIATED CONTENT

### Supporting Information

The Supporting Information is available free of charge at <https://pubs.acs.org/doi/10.1021/acs.analchem.2c03813>.

Description of cell/virus culture, plaque assay, ApoH nanoparticle fabrication, and virus extraction methods; comparison between native ApoH protein and synthetic ApoH peptide; characterization of SARS-CoV-2 primers; optimization of sample collection, preservation, preparation condition, and virus capture protocol; and ApoH assay efficiency on samples with low and high viral loads (PDF)

## AUTHOR INFORMATION

### Corresponding Authors

**Francisco Veas** – Copernicus Integrated Solutions for Biosafety Risks (CISBR), Manguio 34130, France; ApoH-Technologies, La Grande Motte 34280, France; UMR5151/French Research Institute for Development (IRD), University of Montpellier (UM), Montpellier 34093, France; Email: [Francisco.veas@ird.fr](mailto:Francisco.veas@ird.fr)

**Wan Beom Park** – Department of Internal Medicine, Seoul National University College of Medicine, Seoul 03080, Korea; Email: [wbpark1@snu.ac.kr](mailto:wbpark1@snu.ac.kr)

**Sunghoon Kwon** – Interdisciplinary Program in Bioengineering, Seoul National University, Seoul 08826, Korea; Bio-MAX Institute and Department of Electrical and Computer Engineering, Seoul National University, Seoul 08826, Korea; QuantaMatrix Inc., Seoul 08506, Korea; Biomedical Research Institute, Seoul National University Hospital, Seoul 03080, Korea; [orcid.org/0000-0003-3514-1738](https://orcid.org/0000-0003-3514-1738); Email: [skwon@snu.ac.kr](mailto:skwon@snu.ac.kr)

## Authors

- Junwon Kang** – Interdisciplinary Program in Bioengineering, Seoul National University, Seoul 08826, Korea; Integrated Major in Innovative Medical Science, Seoul National University, Seoul 03080, Korea
- Haewook Jang** – Interdisciplinary Program in Bioengineering, Seoul National University, Seoul 08826, Korea
- Tae Hyun Kim** – Bio-MAX Institute and Department of Electrical and Computer Engineering, Seoul National University, Seoul 08826, Korea
- Untack Cho** – QuantaMatrix Inc., Seoul 08506, Korea; Interdisciplinary Program in Cancer Biology, Seoul National University College of Medicine, Seoul 03080, Korea
- Hyeon Bang** – QuantaMatrix Inc., Seoul 08506, Korea
- Jisung Jang** – QuantaMatrix Inc., Seoul 08506, Korea
- Wooseok Lee** – Department of Electrical and Computer Engineering, Seoul National University, Seoul 08826, Korea
- Hyelyn Joo** – Interdisciplinary Program in Bioengineering, Seoul National University, Seoul 08826, Korea
- Jinsung Noh** – Bio-MAX Institute and Department of Electrical and Computer Engineering, Seoul National University, Seoul 08826, Korea
- Gi Yoon Lee** – Department of Electrical and Computer Engineering, Seoul National University, Seoul 08826, Korea
- Dong Hoon Shin** – Department of Internal Medicine, Seoul National University College of Medicine, Seoul 03080, Korea
- Chang Kyung Kang** – Department of Internal Medicine, Seoul National University College of Medicine, Seoul 03080, Korea
- Pyeong Gyun Choe** – Department of Internal Medicine, Seoul National University College of Medicine, Seoul 03080, Korea
- Nam Joong Kim** – Department of Internal Medicine, Seoul National University College of Medicine, Seoul 03080, Korea
- Myoung-don Oh** – Department of Internal Medicine, Seoul National University College of Medicine, Seoul 03080, Korea
- Manki Song** – International Vaccine Institute, Seoul 08826, Korea

Complete contact information is available at:

<https://pubs.acs.org/10.1021/acs.analchem.2c03813>

## Author Contributions

J.K., H.J., and T.H.K. contributed equally to this work. J.K., H.J., T.H.K., F.V., W.B.P., and S.K. conceived and designed the study. J.K., H.J., T.H.K., U.C., and F.V. optimized the protocol for virus capture and viral RNA extraction. U.C., H.B., and J.J. designed the primers for the RT-qPCR assay. W.L., H.J., and M.S. carried out the cell culture for virus cultivation and plaque assay. W.L., H.J., and G.Y.L. performed the live and dead assay. J.K. and J.N. conducted the statistical analysis. D.H.S., C.K.K., P.G.C., and N.J.K. collected and prepared the patient samples. W.B.P. and M.O. provided advice on the clinical data for validation. J.K., H.J., T.H.K., F.V., W.B.P., and S.K. analyzed the data and co-wrote the manuscript. All authors discussed the results and commented on the manuscript.

## Notes

The authors declare the following competing financial interest(s): The work was done in collaboration between QuantaMatrix Inc. and ApoH-Technologies. F.V. is the co-founder and CSO of ApoH-Technologies.

## ACKNOWLEDGMENTS

This research was supported by the Ministry of Science and ICT (MSIT, Republic of Korea), the National Research

Foundation of Korea (NRF-2020R1A3B3079653, NRF-2020R1A2C1007242), the Bio & Medical Technology Development Program of the NRF of Korea (MSIT, 2020M3H1A1073304), BK21 FOUR program of the Education and Research Program for Future ICT Pioneers (Seoul National University in 2021), Seoul National University Bio-MAX Institute (K-BIO KIURI Center, 2020M3H1A1073304), QuantaMatrix Inc., and the Seoul National University Hospital Research Fund (grant no. 0320200330). The pathogen resource (NCCP43326) for this study was provided by the National Culture Collection for Pathogens (Korea National Institute of Health). F.V. acknowledges the ApoH-Technologies' team as well as the European Commission for the European Projects: Horizon 2020 EDCTP "PANDORA-ID-NET" (grant no. RIA2016E-1609) and Horizon Europe "EPIC-Crown-2" (grant no. 101046084).

## REFERENCES

- (1) Adam, D. *Nature* **2022**, *601*, 312–315.
- (2) Baedeker, M.; Ringel, M. S.; Schulze, U. *Nat. Rev. Drug Discov.* **2022**, *21*, 90.
- (3) Harvey, W. T.; Carabelli, A. M.; Jackson, B.; Gupta, R. K.; Thomson, E. C.; Harrison, E. M.; Ludden, C.; Reeve, R.; Rambaut, A.; Peacock, C.; Robertson, U.; Peacock, S. J.; Robertson, D. L. *Nat. Rev. Microbiol.* **2021**, *19*, 409–424.
- (4) Hu, B.; Guo, H.; Zhou, P.; Shi, Z.-L. *Nat. Rev. Microbiol.* **2021**, *19*, 141–154.
- (5) Mercer, T. R.; Salit, M. *Nat. Rev. Genet.* **2021**, *22*, 415–426.
- (6) Kevadiya, B. D.; Machhi, J.; Herskovitz, J.; Oleynikov, M. D.; Blomberg, W. R.; Bajwa, N.; Soni, D.; Das, S.; Hasan, M.; Patel, M.; Senan, A. M.; Gorantla, S.; McMillan, J.; Edagwa, B.; Eisenberg, R.; Gurumurthy, C. B.; Reid, S. P. M.; Punyadeera, C.; Chang, L.; Gendelman, H. E. *Nat. Mater.* **2021**, *20*, 593–605.
- (7) Amaral, C.; Antunes, W.; Moe, E.; Duarte, A. G.; Lima, L. M. P.; Santos, C.; Gomes, I. L.; Afonso, G. S.; Vieira, R.; Teles, H. S. S.; Reis, M. S.; da Silva, M. A. R.; Henriques, A. M.; Fevereiro, M.; Ventura, M. R.; Serrano, M.; Pimentel, C. *Sci. Rep.* **2021**, *11*, 16430.
- (8) Ludwig, K. U.; Schmithausen, R. M.; Li, D.; Jacobs, M. L.; Hollstein, R.; Blumenstock, K.; Liebing, J.; Slabicki, M.; Ben-Shmuel, A.; Israeli, O.; Weiss, S.; Ebert, T. S.; Paran, N.; Rüdiger, W.; Wilbring, G.; Feldman, D.; Lippke, B.; Ishorst, N.; Hochfeld, L. M.; Beins, E. C.; Kaltheuner, I. H.; Schmitz, M.; Wöhler, A.; Döhla, M.; Sib, E.; Jentzsch, M.; Moench, J. D.; Borrajo, J.; Strecker, J.; Reinhardt, B.; Cleary, M.; Geyer, M.; Hölzel, R.; Macrae, M. M.; Nöthen, P.; Hoffmann, M.; Exner, A.; Regev, F.; Zhang, J. L.; Schmid-Burgk, J. L. *Nat. Biotechnol.* **2021**, *39*, 1556–1562.
- (9) Smyrlaki, I.; Ekman, M.; Lentini, A.; Rufino de Sousa, N. R.; Papanicolaou, N.; Vondracek, M.; Aarum, J.; Safari, H.; Muradrasoli, S.; Rothfuchs, A. G.; Albert, J.; Högberg, B.; Reinius, B. *Nat. Commun.* **2020**, *11*, 4812.
- (10) Wyllie, A. L.; Fournier, J.; Casanovas-Massana, A.; Campbell, M.; Tokuyama, M.; Vijayakumar, P.; Warren, J. L.; Geng, B.; Muenker, M. C.; Moore, A. J.; Vogels, C. B. F.; Petrone, M. E.; Ott, I. M.; Lu, P.; Venkataraman, A.; Lu-Culligan, A.; Klein, J.; Earnest, R.; Simonov, M.; Datta, R.; Handoko, R.; Naushad, N.; Sewanan, L. R.; Valdez, J.; White, E. B.; Lapidus, S.; Kalinich, C. C.; Jiang, X.; Kim, D. J.; Kudo, E.; Linehan, M.; Mao, T.; Moriyama, M.; Oh, J. E.; Park, A.; Silva, J.; Song, E.; Takahashi, T.; Taura, M.; Weizman, O.-E.; Wong, P.; Yang, Y.; Bermejo, S.; Odio, C. D.; Omer, S. B.; Cruz, C. S. D.; Farhadian, S.; Martinello, R. A.; Iwasaki, A.; Grubaugh, N. D.; Ko, A. I. *N. Engl. J. Med.* **2020**, *383*, 1283.
- (11) Bloom, J. S.; Sathe, L.; Munugala, C.; Jones, E. M.; Gasperini, M.; Lubock, N. B.; Yarza, F.; Thompson, E. M.; Kovary, K. M.; Park, J.; Marquette, D.; Kay, S.; Lucas, M.; Love, T.; Sina Boeshaghi, A. S.; Brandenburg, O. F.; Guo, L.; Boocock, J.; Hochman, M.; Simpkins, S. W.; Lin, I.; LaPierre, N.; Hong, D.; Zhang, Y.; Oland, G.; Choe, B. J.; Chandrasekaran, S.; Hilt, E. E.; Butte, M. J.; Damoiseaux, R.; Kravitz,



- C.; Cooper, A. R.; Yin, Y.; Pachter, L.; Garner, O. B.; Flint, J.; Eskin, E.; Luo, C.; Kosuri, S.; Kruglyak, L.; Arboleda, V. A. *Nat. Biomed. Eng.* **2021**, *5*, 657–665.
- (12) Marty, F. M.; Chen, K.; Verrill, K. A. *N. Engl. J. Med.* **2020**, *382*, No. e76.
- (13) Goldfarb, D. M.; Tilley, P.; Al-Rawahi, G. N.; Srigley, J. A.; Ford, G.; Pedersen, H.; Pabbi, A.; Hannam-Clark, S.; Charles, M.; Dittrick, M.; Gadkar, V. J.; Pernica, J. M.; Hoang, L. M. N. *J. Clin. Microbiol.* **2021**, *59*, No. e02427-20.
- (14) Alemany, A.; Millat-Martinez, P.; Ouchi, D.; Corbacho-Monné, M.; Bordoy, A. E.; Esteban, C.; Hernández, A.; Casañ, C.; Gonzalez, V.; Costes, G.; Capdevila-Jáuregui, M.; Torrano-Soler, P.; José, A. S.; Ara, J.; Prat, N.; Clotet, B.; Bassat, Q.; Gimenez, M.; Blanco, I.; Baro, B.; Mitjà, O. *J. Infect.* **2021**, *83*, 709.
- (15) Wang, W.; Xu, Y.; Gao, R.; Lu, R.; Han, K.; Wu, G.; Tan, W. *JAMA* **2020**, *323*, 1843–1844.
- (16) Lee, R. A.; Herigon, J. C.; Benedetti, A.; Pollock, N. R.; Denkinger, C. M. *J. Clin. Microbiol.* **2021**, *59*, No. e02881-e20.
- (17) Kojima, N.; Turner, F.; Slepnev, V.; Bacelar, A.; Deming, L.; Kodeboyina, S.; Klausner, J. D. *Clin. Infect. Dis.* **2021**, *73*, No. e3106.
- (18) Gertler, M.; Krause, E.; van Loon, W.; Krug, N.; Kausch, F.; Rohardt, C.; Rössig, H.; Michel, J.; Nitsche, A.; Mall, M. A.; Nikolai, O.; Hommes, F.; Burock, S.; Lindner, A. K.; Mockenhaupt, F. P.; Pison, U.; Seybold, J. *Int. J. Infect. Dis.* **2021**, *110*, 261–266.
- (19) Wölfel, R.; Corman, V. M.; Guggemos, W.; Seilmaier, M.; Zange, S.; Müller, M. A.; Niemeyer, D.; Jones, T. C.; Vollmar, P.; Rothe, C.; Hoelscher, M.; Bleicker, T.; Brünink, S.; Schneider, J.; Ehmann, R.; Zwirgmaier, K.; Drosten, C.; Wendtner, C. *Nature* **2020**, *581*, 465–469.
- (20) Savelle, E. S.; Winnett, A. V.; Romano, A. E.; Porter, M. K.; Shelby, N.; Akana, R.; Ji, J.; Cooper, M. M.; Schlenker, N. W.; Reyes, J. A.; Carter, A. M.; Barlow, J. T.; Tognazzini, C.; Feaster, M.; Goh, Y.-Y.; Ismagilov, R. F. *J. Clin. Microbiol.* **2022**, *60*, No. e0178521.
- (21) Zou, L.; Ruan, F.; Huang, M.; Liang, L.; Huang, H.; Hong, Z.; Yu, J.; Kang, M.; Song, Y.; Xia, J.; Guo, Q.; Song, T.; He, J.; Yen, H.-L.; Peiris, M.; Wu, J. *N. Engl. J. Med.* **2020**, *382*, 1177–1179.
- (22) Areo, O.; Joshi, P. U.; Obrenovich, M.; Tayahi, M.; Heldt, C. L. *Microorganisms* **2021**, *9*, 1606.
- (23) Stohr, J. J. M.; Wennekes, M.; van der Ent, M.; Diederer, B. M. W.; Kluytmans-van den Bergh, M. F. Q. K.; Bergmans, A. M. C.; Kluytmans, J. A. J. W.; Pas, S. D. *J. Clin. Virol.* **2020**, *133*, 104686.
- (24) Ninivaggi, M.; Kelchtermans, H.; Lindhout, T.; de Laat, B. *de Thromb. Res.* **2012**, *130*, S33–S36.
- (25) Wurm, H. *Int. J. Biochem.* **1984**, *16*, 511–515.
- (26) Nakaya, Y.; Schaefer, E. J.; Brewer, H. B. *Biochem. Biophys. Res. Commun.* **1980**, *95*, 1168–1172.
- (27) Nimpf, J.; Bevers, E. M.; Bomans, P. H. H.; Till, U.; Wurm, H.; Kostner, G. M.; Zwaal, R. F. A. *Biochim. Biophys. Acta, Gen. Subj.* **1986**, *884*, 142–149.
- (28) Niessen, H. W.; Lagrand, W. K.; Rensink, H. J.; Meijer, C. J.; Aarden, L.; Hack, C. E.; VisserApolipoprotein, C. H. *J. Clin. Pathol.* **2000**, *53*, 863.
- (29) Vutukuru, M. R.; Sharma, D. K.; Ragavendar, M.; Schmolke, S.; Huang, Y.; Gumbrecht, W.; Mitra, N. *J. Microbiol. Methods* **2016**, *131*, 105–109.
- (30) Stefas, I.; Tigrett, S.; Dubois, G.; Kaiser, M.; Lucarz, E.; Gobby, D.; Bray, D.; Ellerbrok, H.; Zarski, J. P.; Veas, F. *PLoS One* **2015**, *10*, No. e0140900.
- (31) Ganguli, A.; Mostafa, A.; Berger, J.; Aydin, M. Y.; Sun, F.; Ramirez, S. A. S.; Valera, E.; Cunningham, B. T.; King, W. P.; Bashir, R. *Proc. Natl. Acad. Sci. U.S.A.* **2020**, *117*, 22727–22735.
- (32) Sender, R.; Bar-On, Y. M.; Gleizer, S.; Bernshtein, B.; Flamholz, A.; Phillips, R.; Milo, R. *Proc. Natl. Acad. Sci. U.S.A.* **2021**, *118*, No. e2024815118.
- (33) Kerimov, D.; Tamminen, P.; Viskari, H.; Lehtimäki, L.; Aittoniemi, J. *PLoS One* **2021**, *16*, No. e0260184.
- (34) Watson, J.; Whiting, P. F.; Brush, J. E. *BMJ* **2020**, *369*, m1808.
- (35) Alcoba-Florez, J.; Gil-Campesino, H.; Artola, D. G.-M.; González-Montelongo, R.; Valenzuela-Fernández, A.; Ciuffreda, L.; Flores, C. *Int. J. Infect. Dis.* **2020**, *99*, 190–192.
- (36) Jarvis, K. F.; Kelley, J. B. *Sci. Rep.* **2021**, *11*, 9221.
- (37) He, X.; Lau, E. H. Y.; Wu, P.; Deng, X.; Wang, J.; Hao, X.; Lau, Y. C.; Wong, J. Y.; Guan, Y.; Tan, X.; Mo, X.; Chen, Y.; Liao, B.; Chen, W.; Hu, F.; Zhang, Q.; Zhong, M.; Wu, Y.; Zhao, L.; Zhang, F.; Cowling, B. J.; Li, F.; Leung, G. M. *Nat. Med.* **2020**, *26*, 672–675.
- (38) Nicoletis, M. A. L.; Raimundo, R. L. G.; Peixoto, P. S.; Andreazzi, C. S. *Sci. Rep.* **2021**, *11*, 13001.
- (39) Sahin, O.; Yildirmak, T.; Karacalar, S.; Aydın, E.; Ciftci, M. A.; Bagci, H.; Yildirim, S.; Emeklioglu, C.; Balci, B. G.; Genc, S.; Cingillioglu, B.; Mihmanli, V.; Khalil, A.; Kalafat, E. *Int. J. Clin. Pract.* **2021**, *75*, No. e14670.
- (40) Xiao, A. T.; Tong, Y. X.; Zhang, S. *J. Med. Virol.* **2020**, *92*, 1755.
- (41) Cleary, B.; Hay, J. A.; Blumenstiel, B.; Harden, M.; Cipicchio, M.; Bezney, J.; Simonton, B.; Hong, D.; Senghore, M.; Sesay, A. K.; Gabriel, S.; Regev, A.; Mina, M. J. *Sci. Transl. Med.* **2021**, *13*, No. eabf1568.